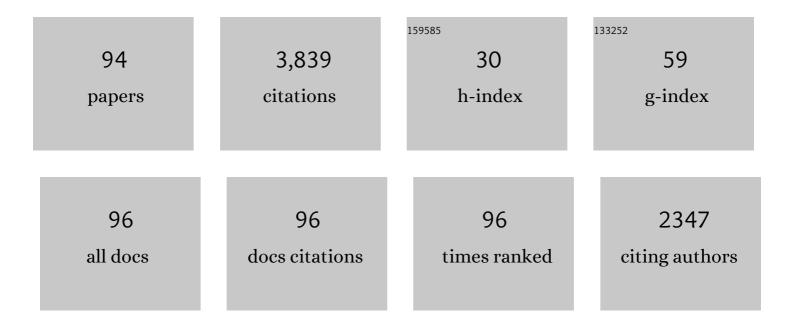
List of Publications by Year in descending order

Source: https://exaly.com/author-pdf/1561562/publications.pdf Version: 2024-02-01



#	Article	IF	CITATIONS
1	On the chances and challenges of combining electronâ€collecting <i>n</i> POLO and holeâ€collecting Alâ€ <i>p</i> <sup>+</sup> contacts in highly efficient <i>p</i> â€type câ€Si solar cells. Progress in Photovoltaics: Research and Applications, 2023, 31, 327-340.	8.1	9
2	Firing stability of tube furnaceâ€annealed nâ€ŧype poly‣i on oxide junctions. Progress in Photovoltaics: Research and Applications, 2022, 30, 49-64.	8.1	12
3	Light and elevated temperature induced degradation and recovery of gallium-doped Czochralski-silicon solar cells. Scientific Reports, 2022, 12, 8089.	3.3	5
4	Simulation-based roadmap for the integration of poly-silicon on oxide contacts into screen-printed crystalline silicon solar cells. Scientific Reports, 2021, 11, 996.	3.3	24
5	Contacting a single nanometerâ€sized pinhole in the interfacial oxide of a polyâ€silicon on oxide (POLO) solar cell junction. Progress in Photovoltaics: Research and Applications, 2021, 29, 936-942.	8.1	5
6	Fully screenâ€printed silicon solar cells with local Alâ€p <sup>+</sup> and nâ€type POLO interdigitated back contacts with a <i>V</i> <sub>OC</sub> of 716 mV and an efficiency of 23%. Progress in Photovoltaics: Research and Applications, 2021, 29, 516-523.	8.1	10
7	Firing-Stable PECVD SiO <i><sub>x</sub></i> N <i><sub>y</sub></i> /n-Poly-Si Surface Passivation for Silicon Solar Cells. ACS Applied Energy Materials, 2021, 4, 4646-4653.	5.1	22
8	A Cross-Country Model for End-Use Specific Aggregated Household Load Profiles. Energies, 2021, 14, 2167.	3.1	6
9	Impact of Local Back-Surface-Field Thickness Variation on Performance of PERC Solar Cells. IEEE Journal of Photovoltaics, 2021, 11, 908-913.	2.5	3
10	Changes in hydrogen concentration and defect state density at the poly-Si/SiOx/c-Si interface due to firing. Solar Energy Materials and Solar Cells, 2021, 231, 111297.	6.2	19
11	For none, one, or two polarities—How do POLO junctions fit best into industrial Si solar cells?. Progress in Photovoltaics: Research and Applications, 2020, 28, 503-516.	8.1	28
12	Ultraâ€Thin Polyâ€Si Layers: Passivation Quality, Utilization of Charge Carriers Generated in the Polyâ€Si and Application on Screenâ€Printed Doubleâ€Side Contacted Polycrystalline Si on Oxide Cells. Solar Rrl, 2020, 4, 2000177.	5.8	21
13	A 22.3% Efficient pâ€Type Back Junction Solar Cell with an Alâ€Printed Frontâ€Side Grid and a Passivating n <sup>+</sup> â€Type Polysilicon on Oxide Contact at the Rear Side. Solar Rrl, 2020, 4, 2000435.	5.8	13
14	Modeling recombination and contact resistance of polyâ€ <b>s</b> i junctions. Progress in Photovoltaics: Research and Applications, 2020, 28, 1289-1307.	8.1	20
15	Evolutionary PERC+ solar cell efficiency projection towards 24% evaluating shadow-mask-deposited poly-Si fingers below the Ag front contact as next improvement step. Solar Energy Materials and Solar Cells, 2020, 212, 110586.	6.2	36
16	Degradation and Regeneration of <i>n</i> <sup>+</sup> -Doped Poly-Si Surface Passivation on <i>p</i> -Type and <i>n</i> -Type Cz-Si Under Illumination and Dark Annealing. IEEE Journal of Photovoltaics, 2020, 10, 423-430.	2.5	17
17	Evaluation of localized vertical current formation in carrier selective passivation layers of silicon solar cells by conductive AFM. AIP Conference Proceedings, 2019, , .	0.4	3
18	Detailed Analysis and Understanding of the Transport Mechanism of Poly-Si-Based Carrier Selective Junctions. IEEE Journal of Photovoltaics, 2019, 9, 1575-1582.	2.5	18

#	Article	IF	CITATIONS
19	Backâ€contacted bottom cells with three terminals: Maximizing power extraction from currentâ€mismatched tandem cells. Progress in Photovoltaics: Research and Applications, 2019, 27, 410-423.	8.1	31
20	High Temperature Annealing of ZnO:Al on Passivating POLO Junctions: Impact on Transparency, Conductivity, Junction Passivation, and Interface Stability. IEEE Journal of Photovoltaics, 2019, 9, 89-96.	2.5	19
21	From PERC to Tandem: POLO- and p <sup>+</sup> /n <sup>+</sup> Poly-Si Tunneling Junction as Interface Between Bottom and Top Cell. IEEE Journal of Photovoltaics, 2019, 9, 49-54.	2.5	29
22	26.1%â€efficient POLOâ€IBC cells: Quantification of electrical and optical loss mechanisms. Progress in Photovoltaics: Research and Applications, 2019, 27, 950-958.	8.1	76
23	Building Blocks for Industrial, Screen-Printed Double-Side Contacted POLO Cells With Highly Transparent ZnO:Al Layers. IEEE Journal of Photovoltaics, 2018, , 1-7.	2.5	19
24	Perimeter Recombination in 25%-Efficient IBC Solar Cells With Passivating POLO Contacts for Both Polarities. IEEE Journal of Photovoltaics, 2018, 8, 23-29.	2.5	49
25	Accurate Calculation of the Absorptance Enhances Efficiency Limit of Crystalline Silicon Solar Cells With Lambertian Light Trapping. IEEE Journal of Photovoltaics, 2018, 8, 1156-1158.	2.5	62
26	Laser contact openings for local poly-Si-metal contacts enabling 26.1%-efficient POLO-IBC solar cells. Solar Energy Materials and Solar Cells, 2018, 186, 184-193.	6.2	475
27	Reassessment of intrinsic lifetime limit in n-type crystalline silicon and implication on maximum solar cell efficiency. Solar Energy Materials and Solar Cells, 2018, 186, 194-199.	6.2	66
28	Surface passivation of crystalline silicon solar cells: Present and future. Solar Energy Materials and Solar Cells, 2018, 187, 39-54.	6.2	285
29	UV-induced degradation of PERC solar modules with UV-transparent encapsulation materials. Progress in Photovoltaics: Research and Applications, 2017, 25, 409-416.	8.1	29
30	Impact of Contacting Geometries When Measuring Fill Factors of Solar Cell Current–Voltage Characteristics. IEEE Journal of Photovoltaics, 2017, 7, 747-754.	2.5	8
31	A Roadmap Toward 24% Efficient PERC Solar Cells in Industrial Mass Production. IEEE Journal of Photovoltaics, 2017, 7, 1541-1550.	2.5	102
32	UV radiation hardness of photovoltaic modules featuring crystalline Si solar cells with AlO <i><sub>x</sub></i> /p <sup>+</sup> â€ŧype Si and SiN <i><sub>y</sub></i> /n <sup>+</sup> â€ŧype Si interfaces. Physica Status Solidi - Rapid Research Letters, 2017, 11, 1700178.	2.4	11
33	On the recombination behavior of p <sup><i>+</i></sup> -type polysilicon on oxide junctions deposited by different methods on textured and planar surfaces. Physica Status Solidi (A) Applications and Materials Science, 2017, 214, 1700058.	1.8	48
34	Junction Resistivity of Carrier-Selective Polysilicon on Oxide Junctions and Its Impact on Solar Cell Performance. IEEE Journal of Photovoltaics, 2017, 7, 11-18.	2.5	91
35	Emitter saturation current densities of 22 fA/cm <sup>2</sup> applied to industrial PERC solar cells approaching 22% conversion efficiency. Progress in Photovoltaics: Research and Applications, 2017, 25, 509-514.	8.1	26
36	Improvement of the SRH bulk lifetime upon formation of n-type POLO junctions for 25% efficient Si solar cells. Solar Energy Materials and Solar Cells, 2017, 173, 85-91.	6.2	65

#	Article	IF	CITATIONS
37	21.0%-efficient co-diffused screen printed n-type silicon solar cell with rear-side boron emitter. Physica Status Solidi - Rapid Research Letters, 2016, 10, 148-152.	2.4	8
38	Recombination Behavior of Photolithography-free Back Junction Back Contact Solar Cells with Carrier-selective Polysilicon on Oxide Junctions for Both Polarities. Energy Procedia, 2016, 92, 412-418.	1.8	42
39	Parasitic Absorption in Polycrystalline Si-layers for Carrier-selective Front Junctions. Energy Procedia, 2016, 92, 199-204.	1.8	77
40	Industrial bifacial n-type silicon solar cells applying a boron co-diffused rear emitter and an aluminum rear finger grid. Physica Status Solidi (A) Applications and Materials Science, 2016, 213, 3046-3052.	1.8	12
41	Contact Selectivity and Efficiency in Crystalline Silicon Photovoltaics. IEEE Journal of Photovoltaics, 2016, 6, 1413-1420.	2.5	140
42	Reuse of Substrate Wafers for the Porous Silicon Layer Transfer. IEEE Journal of Photovoltaics, 2016, 6, 783-790.	2.5	8
43	21.0%-efficient screen-printed n-PERT back-junction silicon solar cell with plasma-deposited boron diffusion source. Solar Energy Materials and Solar Cells, 2016, 158, 50-54.	6.2	15
44	Breakdown of the efficiency gap to 29% based on experimental input data and modeling. Progress in Photovoltaics: Research and Applications, 2016, 24, 1475-1486.	8.1	41
45	Optimized Interconnection of Passivated Emitter and Rear Cells by Experimentally Verified Modeling. IEEE Journal of Photovoltaics, 2016, 6, 432-439.	2.5	23
46	Light Trapping and Surface Passivation of Micron-Scaled Macroporous Blind Holes. IEEE Journal of Photovoltaics, 2016, 6, 397-403.	2.5	4
47	Thermal processes driving laser-welding for module interconnection. , 2015, , .		1
48	Interconnection of busbarâ€free back contacted solar cells by laser welding. Progress in Photovoltaics: Research and Applications, 2015, 23, 1057-1065.	8.1	10
49	Ion Implantation for Poly-Si Passivated Back-Junction Back-Contacted Solar Cells. IEEE Journal of Photovoltaics, 2015, 5, 507-514.	2.5	131
50	Ion implantation of boric molecules for silicon solar cells. Solar Energy Materials and Solar Cells, 2015, 142, 12-17.	6.2	9
51	Directional Heating and Cooling for Controlled Spalling. IEEE Journal of Photovoltaics, 2015, 5, 195-201.	2.5	9
52	Analysis of Thermal Processes Driving Laser Welding of Aluminum Deposited on Glass Substrates for Module Interconnection of Silicon Solar Cells. IEEE Journal of Photovoltaics, 2015, 5, 1606-1612.	2.5	3
53	Notation= 'TeX' >\$inbox{-}V\$ Characteristics of <formula formulatype="inline"&gt;<tex notation="TeX">\$hbox{p}\$</tex> Polycrystalline Si/ <formula formulatype="inline"><tex Notation="TeX"&gt;\$hbox{n}\$</tex </formula> Monocrystalline Si, and <formula< td=""><td>2.5</td><td>91</td></formula<></formula 	2.5	91
54	formulatype="inline">, <,tex Notation="TeX">,\$hbox{n}\$<,/tex>,<,/formula>, P. IEEE 21.2%-efficient fineline-printed PERC solar cell with 5 busbar front grid. Physica Status Solidi - Rapid Research Letters, 2014, 8, 675-679.	2.4	61

#	Article	IF	CITATIONS
55	Emitter recombination current densities of boron emitters with silver/aluminum pastes. , 2014, , .		13
56	Analytical Theory for Extracting Specific Contact Resistances of Thick Samples From the Transmission Line Method. IEEE Electron Device Letters, 2014, 35, 9-11.	3.9	41
57	Laser microwelding of thin Al layers for interconnection of crystalline Si solar cells: analysis of process limits for ns and μs lasers. Journal of Photonics for Energy, 2014, 4, 041597.	1.3	1
58	Epitaxial Si films carried by thick polycrystalline Si as a drop-in replacement for conventional Si wafers. , 2014, , .		0
59	Recombination behavior and contact resistance of n+ and p+ poly-crystalline Si/mono-crystalline Si junctions. Solar Energy Materials and Solar Cells, 2014, 131, 85-91.	6.2	195
60	Lambertian light trapping in thin crystalline macroporous Si layers. Physica Status Solidi - Rapid Research Letters, 2014, 8, 235-238.	2.4	12
61	Direct Laser Texturing for High-Efficiency Silicon Solar Cells. IEEE Journal of Photovoltaics, 2013, 3, 656-661.	2.5	31
62	Aluminum Evaporation and Etching for the Front-Side Metallization of Solar Cells. IEEE Journal of Photovoltaics, 2013, 3, 702-708.	2.5	5
63	Modeling the Spectral Luminescence Emission of Silicon Solar Cells and Wafers. IEEE Journal of Photovoltaics, 2013, 3, 1038-1052.	2.5	38
64	Bow of Silicon Wafers After In-Line High-Rate Evaporation of Aluminum. IEEE Journal of Photovoltaics, 2013, 3, 212-216.	2.5	6
65	Application of a New Ray Tracing Framework to the Analysis of Extended Regions in Si Solar Cell Modules. Energy Procedia, 2013, 38, 86-93.	1.8	45
66	Macroporous Silicon Solar Cells With an Epitaxial Emitter. IEEE Journal of Photovoltaics, 2013, 3, 723-729.	2.5	16
67	Al <sup>+</sup> -doping of Si by laser ablation of Al <sub>2</sub> O <sub>3</sub> /SiN passivation. Physica Status Solidi (A) Applications and Materials Science, 2013, 210, 1871-1873.	1.8	7
68	From highâ€efficiency <i>n</i> â€ŧype solar cells to modules exceeding 20% efficiency with aluminumâ€based cell interconnection. Progress in Photovoltaics: Research and Applications, 2013, 21, 1354-1362.	8.1	3
69	Al-Foil on Encapsulant for the Interconnection of Al-Metalized Silicon Solar Cells. IEEE Journal of Photovoltaics, 2013, 3, 77-82.	2.5	12
70	Optimizing the geometry of local aluminum-alloyed contacts to fully screen-printed silicon solar cells. , 2012, , .		5
71	Macroporous silicon as an absorber for thin heterojunction solar cells. , 2012, , .		2
72	Simulation Tool for Equivalent Circuit Modeling of Photovoltaic Devices. IEEE Journal of Photovoltaics, 2012, 2, 572-579.	2.5	32

ROLF BRENDEL

#	Article	IF	CITATIONS
73	19%â€efficient and 43 µmâ€thick crystalline Si solar cell from layer transfer using porous silicon. Progress in Photovoltaics: Research and Applications, 2012, 20, 1-5.	8.1	236
74	Modeling solar cells with the dopantâ€diffused layers treated as conductive boundaries. Progress in Photovoltaics: Research and Applications, 2012, 20, 31-43.	8.1	74
75	Towards 20% efficient largeâ€area screenâ€printed rearâ€passivated silicon solar cells. Progress in Photovoltaics: Research and Applications, 2012, 20, 630-638.	8.1	100
76	Modeling the formation of local highly aluminum-doped silicon regions by rapid thermal annealing of screen-printed aluminum. Physica Status Solidi - Rapid Research Letters, 2012, 6, 111-113.	2.4	19
77	Thin macroporous silicon heterojunction solar cells. Physica Status Solidi - Rapid Research Letters, 2012, 6, 187-189.	2.4	24
78	Aluminum-Based Mechanical and Electrical Laser Interconnection Process for Module Integration of Silicon Solar Cells. IEEE Journal of Photovoltaics, 2012, 2, 16-21.	2.5	20
79	19% Efficient Thin-Film Crystalline Silicon Solar Cells From Layer Transfer Using Porous Silicon: A Loss Analysis by Means of Three-Dimensional Simulations. IEEE Transactions on Electron Devices, 2012, 59, 909-917.	3.0	10
80	Contact resistance of local rear side contacts of screen-printed silicon PERC solar cells with efficiencies up to 19.4%. , 2011, , .		2
81	High-rate atomic layer deposition of Al2O3 for the surface passivation of Si solar cells. Energy Procedia, 2011, 8, 301-306.	1.8	60
82	High Efficiency N-Type Emitter-Wrap-Through Silicon Solar Cells. IEEE Journal of Photovoltaics, 2011, 1, 49-53.	2.5	34
83	High-Efficiency Cells From Layer Transfer: A First Step Toward Thin-Film/Wafer Hybrid Silicon Technologies. IEEE Journal of Photovoltaics, 2011, 1, 9-15.	2.5	23
84	19.4%â€efficient largeâ€area fully screenâ€printed silicon solar cells. Physica Status Solidi - Rapid Research Letters, 2011, 5, 147-149.	2.4	111
85	Contact passivation in silicon solar cells using atomicâ€layerâ€deposited aluminum oxide layers. Physica Status Solidi - Rapid Research Letters, 2011, 5, 298-300.	2.4	65
86	Laser transfer doping for contacting n-type crystalline Si solar cells. Physica Status Solidi (A) Applications and Materials Science, 2011, 208, 1964-1966.	1.8	7
87	High efficiency n-type emitter-wrap-through silicon solar cells. , 2011, , .		2
88	Modelling c‣i/SiN <i><sub>x</sub></i> interface recombination by surface damage. Physica Status Solidi - Rapid Research Letters, 2010, 4, 91-93.	2.4	9
89	Large area macroporous silicon layers for monocrystalline thin-film solar cells. , 2010, , .		3
90	Influence of emitter profile characteristics on thermal stability and passiviation quality of a-Si/SiN <inf>X</inf> -passivated boron emitters. , 2010, , .		3

#	Article	IF	CITATIONS
91	Rear-side point-contacts by inline thermal evaporation of aluminum. , 2010, , .		10
92	Simulation of optical properties of Si wire cells. , 2009, , .		3
93	Numerical simulations of buried emitter backâ€junction solar cells. Progress in Photovoltaics: Research and Applications, 2009, 17, 253-263.	8.1	15
94	The origin of reduced fill factors of emitter-wrap-through-solar cells. Physica Status Solidi - Rapid Research Letters, 2008, 2, 251-253.	2.4	12